

Dartmouth College

## Dartmouth Digital Commons

---

Computer Science Technical Reports

Computer Science

---

2023

### Reasoning about the Conant Gasket

M. Douglas McIlroy

*Dartmouth College*, [douglas.mcilroy@dartmouth.edu](mailto:douglas.mcilroy@dartmouth.edu)

Follow this and additional works at: [https://digitalcommons.dartmouth.edu/cs\\_tr](https://digitalcommons.dartmouth.edu/cs_tr)



Part of the [Computer Sciences Commons](#)

---

#### Dartmouth Digital Commons Citation

McIlroy, M. Douglas, "Reasoning about the Conant Gasket" (2023). Computer Science Technical Report TR2023-1003. [https://digitalcommons.dartmouth.edu/cs\\_tr/385](https://digitalcommons.dartmouth.edu/cs_tr/385)

This Technical Report is brought to you for free and open access by the Computer Science at Dartmouth Digital Commons. It has been accepted for inclusion in Computer Science Technical Reports by an authorized administrator of Dartmouth Digital Commons. For more information, please contact [dartmouthdigitalcommons@groups.dartmouth.edu](mailto:dartmouthdigitalcommons@groups.dartmouth.edu).

# Reasoning about the Conant Gasket

*M. Douglas McIlroy*

Dartmouth College, Department of Computer Science  
Technical report TR2023-1003

## ABSTRACT

Previously conjectured properties of the Conant gasket, a particular non-periodic tiling of the non-negative integer grid, are proved using new recurrences. A slabwise periodicity property is identified and proved. Further fractal properties are conjectured.

A Conant gasket,  $G_n$ , is a particular configuration of vertical and horizontal unit segments drawn between adjacent points in the non-negative integer grid, as illustrated in Figure 2. The union (also the limit as  $n$  goes to infinity) of all  $G_n$  constitutes a tiling of the first quadrant by rectangles. The number of facets in  $G_n$  is enumerated by an integer sequence defined at [OEIS, A328080]. Conant’s original sequence and its properties are more fully discussed at [OEIS, A328078].\* I am not aware of any pertinent peer-reviewed literature. The main contribution of this note is an algebraic description of the Conant gasket. The description yields an elegant program for constructing the figure and a formalism for proving conjectures that fairly leap out of pictures like Figure 2. Conjectures about transposition and “ruler ticks” posted at [OEIS, A328078] are proved, as is a new theorem about periodicity. Finally, conjectures about fractal properties are offered, in particular about the taxonomy of facet shapes and the appearance of patches of symmetry.

## 1. Construction and algebraic formulation

The following construction creates even generations of the original Conant sequence of figures. Its relation to the full sequence is more fully described in Section 3.1.

Coordinate values in  $G_n$  range from 0 through  $2^n$ .  $G_0$  is a unit square. This recipe, illustrated in Figure 1, generates  $G_{n+1}$  from  $G_n$ :

- Magnify  $G_n$  by doubling coordinate values.
- Weave  $2^n$  odd verticals from bottom to top.
- Weave  $2^n$  odd horizontals from left to right.

Terms used in the recipe and in subsequent discussion are defined as follows.

An *odd vertical* is a vertical line at an odd horizontal coordinate. *Even vertical* and *odd/even horizontal* are defined similarly.

---

\* A prior description has been said to be available to Facebook patrons at <https://www.facebook.com/groups/20666497429>.

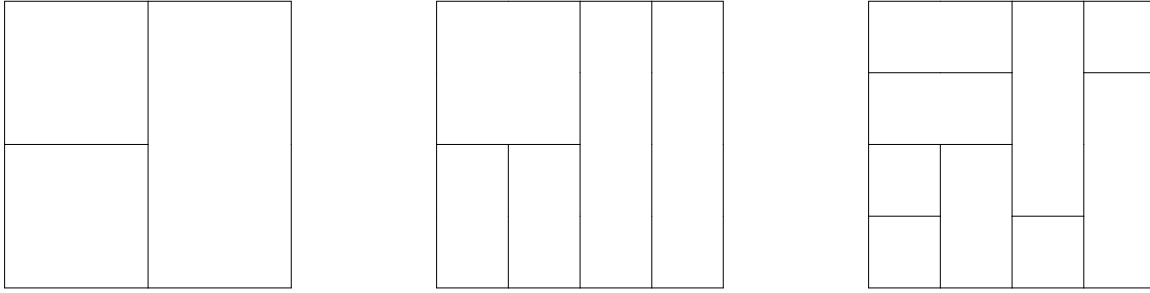


Figure 1. Left:  $G_1$  magnified by a factor of 2. Center: after weaving odd verticals. Right: after weaving odd horizontals to complete  $G_2$ .

To *weave* a vertical, trace the line from bottom to top beginning with with pen down, then alternately raise and lower the pen upon encountering horizontal bars. Horizontals are woven similarly from left to right, alternating at vertical bars.

A *bar* is a closed unit segment drawn with pen down. Other unit segments are called *gaps*. Magnification turns one segment into two.

A *facet* is a region bounded by bars, with no bars in the interior. Facets are necessarily rectangular.

A segment between point  $(i, j)$  and  $(i, j + 1)$  is said to *emanate from* point  $(i, j)$  or from horizontal  $j$  and to *encounter* horizontal  $j + 1$ . Similarly a segment between  $(i, j)$  and  $(i + 1, j)$  emanates from  $(i, j)$  or from vertical  $i$  and encounters vertical  $j + 1$ .

The construction produces a unit square at the origin in every  $G_n$ . This unit square is subsequently treated in exactly the same way as  $G_0$  was. By induction  $G_n$  contains  $G_k$  for  $0 \leq k \leq n$ .

Define functions  $v(i, j)$  and  $h(i, j)$  on points  $(i, j)$  of the grid to have value 1 if a vertical bar or horizontal bar respectively emanates from  $(i, j)$ , otherwise 0. Formulas (1) and (3) below describe the magnifying step; (2) and (4) describe the two weaving steps.

*Notation.* In formulas (1)-(4) and throughout this note,  $/$  is the integer quotient operator. Sums of  $v$  and  $h$  values are taken mod 2.\*

$$v(i, j) = v(i/2, j/2), \quad i \text{ even} \quad (1)$$

$$v(i, j) = \sum_{k=0}^{j/2} h(i, 2k), \quad i \text{ odd} \quad (2)$$

$$h(i, j) = h(i/2, j/2), \quad j \text{ even} \quad (3)$$

$$h(i, j) = \sum_{k=0}^i v(k, j), \quad j \text{ odd} \quad (4)$$

Formulas (1)-(4) define a transformation,  $C$  (for Conant), from values on the grid to values on the grid. Although  $C$  was motivated by construction of  $G_{n+1}$  from  $G_n$ , it in fact applies to the whole first quadrant. The limit,  $G$ , of the iteration  $G_{n+1} = C(G_n)$  is a

\* Equivalently one may understand  $v$  and  $h$  as Boolean-valued functions and addition of Booleans as exclusive-or. Program 1 is written in these terms.

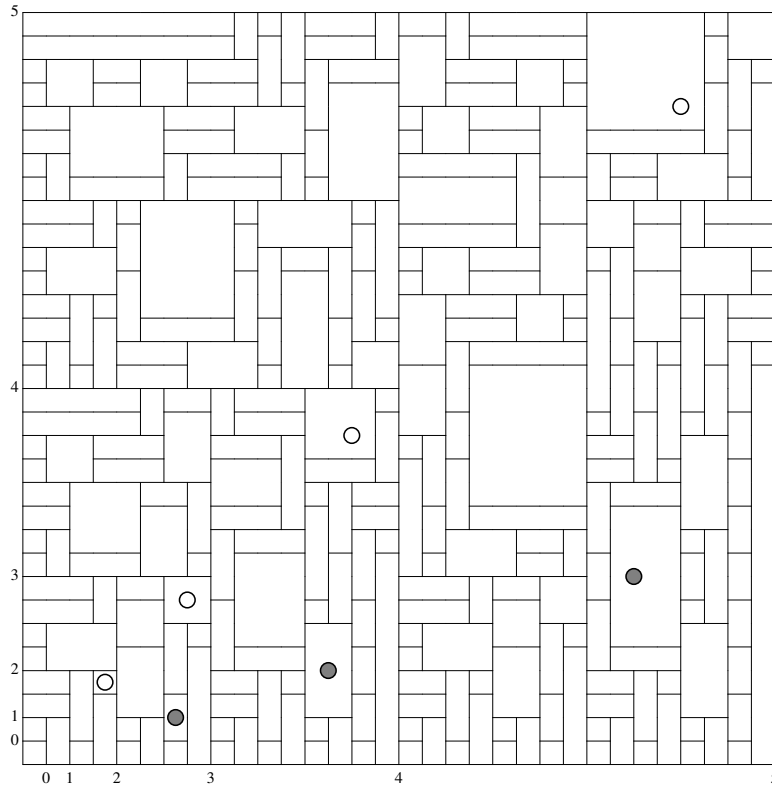


Figure 2. Conant gasket  $G_5$ . The outer boundary of each contained  $G_n$  is marked  $n$ . Circular symbols identify facet families described in Section 6.

configuration that contains  $G_n$  for all  $n$ . In other words,  $G$ —the ultimate Conant gasket—is the fixed point of  $C$  that contains  $G_0$ . Further inspection reveals that the initial condition can be reduced to specifying only that two bars emanate from  $(0,0)$ .

To simplify computation, sums in equations (2) and (4) may be rewritten inductively.\*

$$v(i, j) = v(i, j - 2) + h(i, 2(j/2))$$

$$\stackrel{(3)}{=} v(i, j - 2) + h(i/2, j/2), \quad i \text{ odd} \tag{5}$$

$$h(i, j) = h(i - 1, j) + v(i, j), \quad j \text{ odd} \tag{6}$$

In a notation that we shall use often, “(3)” above “=” in (5) refers to a formula that justifies the equivalence.

Arguments  $j - 2$  and  $i - 1$  in (5) and (6) can fall below the lower limits of the sums in (2) and (4). Accordingly we define

$$v(i, -2) = 0 \tag{7}$$

$$v(i, -1) = 0 \tag{8}$$

$$h(-1, j) = 0 \tag{9}$$

Program 1 uses these conventions.

---

\* Use of  $h(i/2, j/2)$  instead of  $h(i, 2(j/2))$  in (5) eliminates the dependence of  $v(i, j)$  on  $h(i, j)$  when  $i$  is odd and  $j$  is even, allowing one to compute  $h(i, j)$  after  $v(i, j)$  regardless of the values of  $i$  and  $j$ .

Program 1. This C99 [C99] program constructs an initial  $m \times n$  portion of the infinite Conant gasket. Function *conant* calculates Boolean fields addressed as  $v(i, j)$  and  $h(i, j)$  for  $-1 \leq i \leq m$  and  $-2 \leq j \leq n$ . To provide negative indices, the origin of array  $G$  is offset from that of an underlying array, *base*.

```
#define N 15 /* upper bound: m,n <= 2**N */
struct {
    _Bool v:1;
    _Bool h:1;
} base[(1<<N)+2][(1<<N)+3];
#define G(i,j) base[(i)+1][(j)+2]
#define v(i,j) G(i,j).v
#define h(i,j) G(i,j).h
#define even(n) (n&1) == 0
void conant(int m, int n) {
    int i, j;
    v(0,0) = h(0,0) = 1;
    for(i=0; i<=m; i++)
        for(j=0; j<=n; j++) {
            v(i,j) = even(i)? v(i/2,j/2): v(i,j-2) ^ h(i/2,j/2);
            h(i,j) = even(j)? h(i/2,j/2): h(i-1,j) ^ v(i,j);
        }
}
```

## 2. Selected values

Throughout this section  $i, j$  and  $n$  range over the nonnegative integers unless otherwise stated.

In the limit as  $n$  goes to infinity, the original construction implies that the edges of the first quadrant are marked by continuous lines. This property is reproduced by calculation. Repeated use of (1) and (3) respectively equate  $v(0, j)$  to  $v(0, 0) = 1$  and  $h(i, 0)$  to  $h(0, 0) = 1$ .

$$v(0, j) = 1 \quad (10)$$

$$h(i, 0) = 1 \quad (11)$$

We may also confirm that the construction produces “tick marks”—bars at integer coordinates—perpendicular to both edges of  $G$ . If  $i$  is even and greater than 0, repeated use of (1) shows that  $v(i, 0) = v(k, 0)$  for some odd  $k$ . If  $i$  is odd, (2) and (11) show that  $v(i, 0) = h(i/2, 0) = 1$ . Similar reasoning about  $h(0, j)$  with (3) and (4), completes the proof of

$$v(i, 0) = 1 \quad (12)$$

$$h(0, j) = 1 \quad (13)$$

Because the vertical through  $(i, j)$  with  $j$  odd is drawn before the horizontal through the same point, vertical bars come in even-odd pairs, as do vertical gaps. Horizontal pairing is confined to even horizontals, including, trivially, horizontal 0, on which every segment is a bar.

$$v(i, 2j) = v(i, 2j + 1) \quad (14)$$

$$h(2i, 2j) \stackrel{(3)}{=} h(2i + 1, 2j) \quad (15)$$

To verify (14) algebraically, apply (1) to both sides if  $i$  is even; apply (2) if  $i$  is odd. In particular  $v(i, 1) = v(i, 0)$ , which by (12) is 1.

$$v(i, 1) = 1 \tag{16}$$

It is easy to calculate the distribution of bars on the infinite verticals and horizontals at the outer edges of  $G_n$  for all  $n$ , as marked in Figure 2. Apply (3)  $n$  times to reduce  $h(i, 2^n)$  to  $h(i/2^n, 1)$ . Then

$$h(i, 2^n) \stackrel{(1)}{=} h(i/2^n, 1) \stackrel{(4)}{=} \sum_{k=0}^{i/2^n} v(k, 1) \stackrel{(16)}{=} \sum_{k=0}^{i/2^n} 1 = i/2^n + 1$$

Taken modulo 2,  $i/2^n$  is the same as the  $2^n$ 's bit of the binary representation of  $i$ , which we call  $\text{bit}(n, i)$ .

$$h(i, 2^n) = \text{bit}(n, i) + 1 \tag{17}$$

In other words, length- $2^n$  intervals of bars and gaps alternate on horizontal  $2^n$ .

For segments on the produced right edge of  $G_n$ ,  $n$ -fold use of (1) reduces  $v(2^n, j)$  to

$$v(1, j/2^n) \stackrel{(2)}{=} \sum_{k=0}^{j/2^{n+1}} h(0, k) \stackrel{(13)}{=} \sum_{k=0}^{j/2^{n+1}} 1 = j/2^{n+1} + 1 \pmod{2}$$

Whence

$$v(2^n, j) = \text{bit}(n + 1, j) + 1 \tag{18}$$

For even  $i$ ,  $v(i, 2) \stackrel{(1)(16)}{=} 1$ . For odd  $i$ ,  $v(i, 2)$  satisfies

$$v(i, 2) \stackrel{(5)}{=} v(i, 0) + h(i/2, 1) \stackrel{(12)}{=} 1 + h(i/2, 1)$$

and thus alternates between 0 and 1 per (17). Interleaving values 1,1 for even  $i$  with 0,1 for odd  $i$  creates a repeating pattern: 1,0,1,1.

$$v(i, 2) = \begin{cases} 0, & i = 1 \pmod{4} \\ 1, & \text{otherwise} \end{cases} \tag{19}$$

### 3. Transpose and stretch

Neil Sloane observed that  $G_n$  transposed about the diagonal through (0,0) and stretched vertically by a factor of 2 becomes the left half of  $G_{n+1}$  with odd horizontals absent; see Figure 3. We shall see that similarly transposing and stretching that left half produces  $G_{n+1}$  with odd verticals absent.

In algebraic terms, Sloane's conjecture is

$$v(i, j) = h(j, 2i) \tag{20}$$

$$h(i, j) = v(j, 2i) \stackrel{(14)}{=} v(j, 2i + 1) \tag{21}$$

(20) and (21) hold according to (10) and (11) when either  $i$  or  $j$  is 0. Otherwise, assume (20) and (21) hold at all  $(i, j)$  distinct from  $(i', j')$  where  $0 \leq i \leq i'$  and  $0 \leq j \leq j'$ .

If  $i'$  is even, (20) holds at  $(i', j')$  because the two sides may be reduced thus

$$v(i', j') \stackrel{(1)}{=} v(i'/2, j'/2)$$

$$h(j', 2i') \stackrel{(3)}{=} h(j'/2, i')$$

to values that have been assumed equal. If  $i'$  is odd, the reductions

$$v(i', j') \stackrel{(2)}{=} \sum_{k=0}^{j'} h(i', 2k) \stackrel{(3)}{=} \sum_{k=0}^{j'/2} h(i'/2, k)$$

$$h(j', 2i') \stackrel{(3)}{=} h(j'/2, i') \stackrel{(4)}{=} \sum_{k=0}^{j'/2} v(k, i')$$

yield sums whose corresponding terms have been assumed equal according to (21). This completes the proof of (20). (21) may be proved similarly by case analysis on  $j'$ .

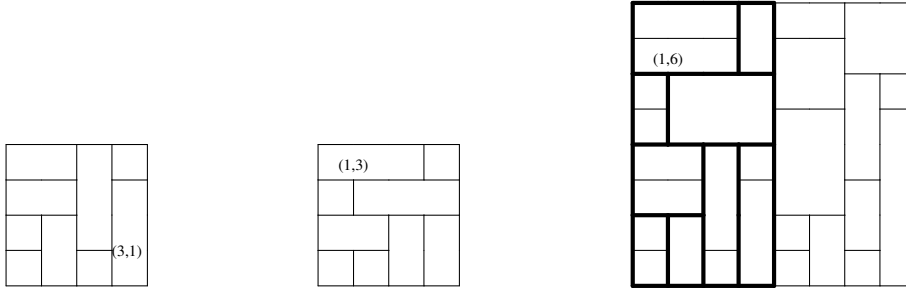


Figure 3. Transpose and stretch. Left:  $G_2$ . Middle:  $G_2$  transposed. Right:  $G_3$ ; thick segments are a vertically stretched copy of the middle image. The transformation of a sample point is indicated. In the notation of Section 3.1 the middle figure is  $T(G_2)$ , and the thick segments in the right image are  $(T ; S_v)(G_2)$ .

As a consequence of the transpose-and-stretch relation, the sequence of facet widths along the left edge of  $G$  is the same as the sequence of facet heights along the bottom edge, with every facet twinned.

### 3.1. Relationship to Conant’s original sequence

We shall develop a non-alternating formula for Conant’s original sequence, in which figures with newly woven verticals (but not horizontal) occur between successive  $G_n$ ’s.

Let  $M$ ,  $W_v$ , and  $W_h$  denote the three steps that make up  $C$ : magnification, vertical weave, and horizontal weave. In these terms,  $C$  may be written

$$C = M ; W_v ; W_h$$

The operator-composition symbol “;” (borrowed from relational algebra) may be read as “then”. The composite operation applies the composed operators in left-to-right order.

Magnification can be decomposed into a horizontal stretch  $S_h$  followed by a vertical stretch  $S_v$ .

$$C = S_h ; S_v ; W_v ; W_h$$

Because  $S_v$  and  $W_v$  commute, we can arrange operations so stretches occur “just in time” for the weaves.

$$C = S_h ; W_v ; S_v ; W_h = (S_h ; W_v) ; (S_v ; W_h) \tag{22}$$

The first and second parenthesized pairs in (22) may be identified as recipes for Conant’s odd and even generations respectively.

Transformation (22) is unchanged if we transpose the figure before performing the first stretch-weave pair and then transpose back. When the figure is transposed, the directions of stretch and weave reverse. Transposition is denoted  $T$ .

$$C = (T ; S_v ; W_h ; T) ; (S_v ; W_h)$$

Change the association of operations

$$C = (T ; S_v ; W_h)^2 = Q^2$$

where  $Q$  denotes the indicated functional square root of  $C$ .

The explanation of Figure 3 reveals that the left half of  $G_{n+1}$  is exactly  $Q(G_n)$ . If we call the left half  $H_{n+1}$ , then the sequence  $Q^k(G_0)$  for  $k = 0, 1, 2, \dots$  is

$$G_0, H_1, G_1, H_2, G_2, \dots \tag{23}$$

As each figure is contained in its successor, the limit  $G$  is the fixed point of  $Q$  that contains  $G_0$ .

Conant's original sequence is the same as (23) with odd-numbered generations transposed. Thus Conant's  $2n - 1$ st generation is  $T(H_n)$ . Since  $T^2$  is the identity transform, Conant's  $k$ th generation may be expressed as  $(Q^k ; T^k)(G_0)$ .

#### 4. Periodicity

Let  $S_n$  be the horizontal slab in  $G$  comprising grid points  $(i, j)$  for  $0 \leq j \leq 2^n$  and segments that emanate from those points; see Figure 4. (The notation  $S_n$  is not related to  $S_h$  and  $S_v$  in Section 3.) Notice that while  $S_n$  contains  $G_n$  and their heights ( $j$ -ranges) are the same, vertical segments that emanate from points  $(i, 2^n)$  belong to  $S_n$  but fall outside  $G_n$ .

*Periodicity theorem.* In  $S_n$ ,  $v(i, j)$  and  $h(i, j)$  are periodic in  $i$  with period  $2^{n+1}$ .

In other words, if  $0 < j \leq 2^n$ , then at most the least significant  $n + 1$  bits of  $i$  are germane in computing  $v(i, j)$  and  $h(i, j)$ . Also, by the periodicity corollary below, if  $0 < i \leq 2^n$ , then at most the least significant  $n + 2$  bits of  $j$  are germane.\* If either  $i$  or  $j$  is zero,

$$v(i, j) = h(i, j) \stackrel{(10)(11)}{=} 1$$

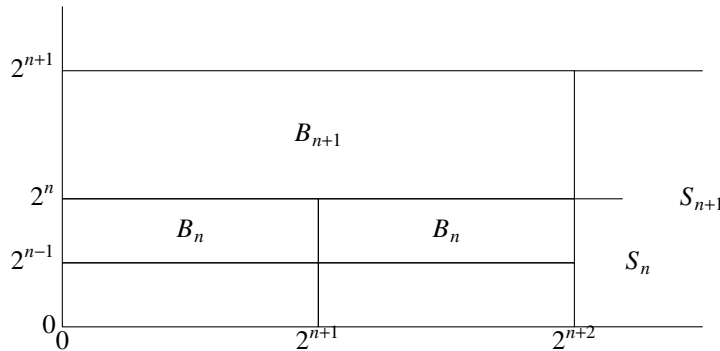


Figure 4. Nomenclature for periodicity theorem. Slabs  $S_n$  and  $S_{n+1}$  begin at the left edge. Left and top boundaries of blocks  $B_n$  and  $B_{n+1}$  belong to the blocks; right and bottom boundaries do not.

The theorem holds for  $n = 0$ : (11), (12) and (16) establish period 1 (hence also period 2) for all functions except  $h(i, 1)$ , which has period 2 per (17).

\* A slight refinement: according to (14), the value of  $v(i, j)$  does not depend on the least significant bit of  $j$ .



The theorem also holds for  $n = 1$ :  $h(i, 2)$  has period 4 per (17), as does  $v(i, 2)$  per (19).

The “even skeleton”—all even-vertical or even-horizontal segments—of slab  $S_{n+1}$  produced by doubling  $S_n$  necessarily has twice the period of  $S_n$ , as do odd verticals woven in this skeleton. Odd horizontals are a different story. In fact, they have the same period, but only because they happen to “get off on the same foot” in the second period as in the first, i.e.

$$h(2^{n+1}, j) = h(0, j) \stackrel{(13)}{=} 1, \quad 0 \leq j \leq 2^n \tag{24}$$

The first equality in (24) remains to be proved. Equivalently, the final segment of an odd horizontal  $j$  in  $B_n$  ought to be a gap:

$$h(2^{n+1} - 1, j) \stackrel{(6)}{=} h(2^{n+1}, j) - v(2^{n+1}, j) \stackrel{(24)(18)}{=} 0$$

That  $h(2^{n+1} - 1, j)$  is indeed a gap is confirmed by the following lemmas. The lemmas depend on each other. They have been separated to untangle the proof, but can be justified by mutual induction.

*Vertical-bar lemma.* The numbers of odd-vertical bars and all vertical bars that encounter or emanate from each horizontal in  $B_n$ , where  $n > 1$  is even, except the number of all vertical bars that emanate from horizontal  $2^n$  is odd.

$$\sum_{i=0}^{2^n-1} v(2i + 1, j) = 0 \tag{25}$$

$$\sum_{i=0}^{2^{n+1}-1} v(i, j) = 0, \quad j < 2^n \tag{26}$$

$$\sum_{i=0}^{2^{n+1}-1} v(i, 2^n) = 1 \tag{27}$$

The truth of the lemma for  $B_2$  follows from enumerating  $v(i, j)$  throughout the block; see Table 1.

Table 1. Counting bars in block  $B_2$ . Values of  $v(i, j)$  and  $h(i, j)$  are read from Figure 2.

$i$	0	1	2	3	4	5	6	7	number of 1s	
$j$	$v(i, j)$								odd $i$	all $i$
3	1	0	1	1	1	0	1	1	2	6
4	1	1	0	0	1	0	1	1	2	5

For larger  $n$ , doubling causes the number of even-vertical bars emanating from even horizontal  $2j$  in the even skeleton of  $B_{n+1}$  to be the same as the number of all vertical bars that emanate from horizontal  $j$  in  $B_n$  and hence to be even or odd according as  $j < 2^n$  or  $j = 2^n$ . The number of even vertical bars that encounter the first even horizontal is even because  $B_{n+1}$  sits atop two copies of  $B_n$ . Every bar emanating from one copy has a twin that emanates from the other.

For the same reason the number of odd-vertical bars that encounter the first even horizontal in  $B_{n+1}$  is even. Because odd verticals are drawn before odd horizontals their parity does not change at odd horizontals. The number of odd verticals that change parity at any even horizontal in  $B_{n+1}$  is the same as the number of even-odd pairs of bars on that

horizontal, which is even according to the horizontal-bar lemma below. Thus the parities of the number of odd-vertical bars that encounter or emanate from every even horizontal in  $B_{n+1}$  is the same:

$$\begin{aligned} \sum_{i=0}^{2^n-1} v(2i+1, j) &\stackrel{(5)}{=} \sum_{i=0}^{2^n-1} (v(2i+1, j-2) + h(i, j/2)) \\ &\stackrel{(14)}{=} \sum_{i=0}^{2^n-1} v(2i+1, j-1) + \sum_{i=0}^{2^n-1} h(i, j/2) \\ &\stackrel{(28)}{=} \sum_{i=0}^{2^n-1} v(2i+1, j-1) \end{aligned}$$

Because an even number of odd-vertical bars encounters the first even horizontal in  $B_{n+1}$ , the number encountering or emanating from every horizontal is even. This completes the proof of the vertical-bar lemma.

*Horizontal-bar lemma.* The numbers of horizontal bars and of even-odd pairs of horizontal bars on horizontal  $j$  in block  $B_n$ , where  $n > 1$ , is even

$$\sum_{i=0}^{2^n-1} h(i, j) = 0 \tag{28}$$

According to (15), even-horizontal bars occur in even-odd pairs. Doubling of even horizontal  $j$  in  $B_n$  to make horizontal  $2j$  produces an even number of pairs and *a fortiori* an even number of bars on horizontal  $2j$ .

The number of horizontal bars on odd horizontal  $j$  is given by

$$\sum_{i=0}^{2^{n+1}-1} h(i, j) \stackrel{(4)}{=} \sum_{i=0}^{2^{n+1}-1} \sum_{k=0}^i v(k, j) = \sum_{k=0}^{2^{n+1}-1} \sum_{i=k}^{2^{n+1}-1} v(k, j) = \sum_{k=0}^{2^{n+1}-1} (2^{n+1} - k)v(k, j)$$

When  $k$  is even, the last summand is even and does not contribute to the parity of the sum. Thus the parity of the sum is the same as the parity of odd-vertical bars that emanate from the horizontal, which is even according to (25). This completes the proof of the horizontal-bar lemma.

With an even number of vertical bars crossing odd horizontals in  $B_n$  per the vertical-bar lemma, the final horizontal segment on an odd horizontal must be a gap. This completes the proof of the periodicity theorem.

The pattern of a transposed and stretched periodic slab is periodic vertically. Odd horizontals drawn to complete the picture necessarily have the same vertical periodicity. Thus we have

*Periodicity corollary.* A vertical slab of width  $2^n$  at the left edge of  $G$  is periodic in  $j$  with period  $2^{n+2}$ .

Could a horizontal or vertical slab with origin (0,0) and thickness  $2^n$  have a period shorter than  $2^{n+1}$  or  $2^{n+2}$  respectively? The answer is no, witness (17) and (18).

## 5. Ruler ticks

Sloane called attention to a “ruler-tick” pattern of facets along the bottom edge of  $G$ ; see Figure 5. The height of the tick preceding an odd vertical is 1. The height of the tick preceding a positive even vertical  $2i$  is  $d(i) + 1$ , where  $d(i)$  is the largest power of 2 that is a divisor of  $i$ . This sequence is given in [OEIS, A330569]. An alternate characterization is

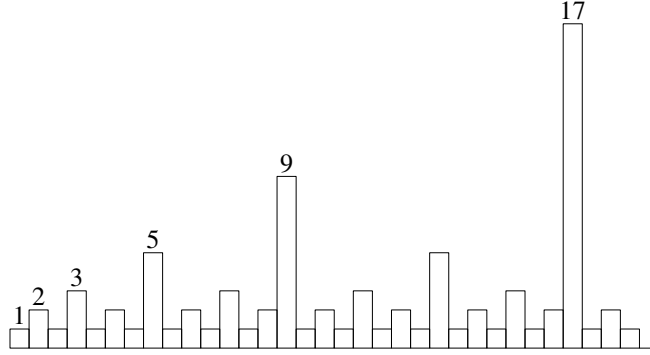


Figure 5. Ruler-tick facets along the bottom edge of  $G$ .

that a ruler tick of height  $2^n + 1$  occupies the right end of a period of slab  $S_n$ .

In Section it was shown that the final segment on every horizontal in block  $B_n$  is a gap. On even horizontals, where gaps come in pairs, the previous segment is also a gap. Thus, when the odd vertical  $2^{n+1} - 1$  is drawn it encounters no horizontal bars in slab  $S_n$  and forms a continuous left side for a facet of height  $2^n + 1$ . The right side of the facet, vertical  $2^{n+1}$ , is also continuous per (18).

Ticks are capped at height  $2^n + 1$ .

$$h(2^{n+1} - 1, 2^n + 1) \stackrel{(4)}{=} \sum_{i=0}^{2^{n+1}-1} v(i, 2^n + 1) \stackrel{(14)}{=} \sum_{i=0}^{2^{n+1}-1} v(i, 2^n) \stackrel{(27)}{=} 1$$

## 6. Facet shapes and families

The sequence,  $R$ , of increasing ruler-facet heights, where

$$R = R_0, R_1, \dots, R_k, \dots = 1, 2, \dots, 2^{k-1} + 1, \dots, \quad k \geq 1$$

plays a pervasive role in facet dimensions. A complete survey of  $G_{15}$  reveals that every facet dimension is  $R_k$  or  $2R_k$  for some  $k$ . Each facet falls into one of the following shape classes. In each class the horizontal dimension is given first.

$$\begin{aligned} &1 \times R_k, \quad 2 \times R_k, \quad R_k \times 1, \quad R_k \times 2, \quad R_k \times R_k, \quad R_k \times 2R_k, \\ &R_{k+1} \times 2R_k, \quad R_k \times R_{k+1}, \quad 2R_k \times R_{k+2} \end{aligned} \tag{29}$$

The classification is unambiguous except for some facets with a side of length 2 or less that is not a member of a family.

Shape classes are embodied in *families* of facets, successive members of which appear in similar positions in successive gaskets  $G_n$  indexed by  $n$ . Successive sizes are indexed by  $k$  within the class. The “similar positions” are witnessed by a *seed* location  $(x, y)$  such that the  $m$ th member of the family counted from 0 contains  $(2^m x, 2^m y)$ .

In Figure 2 solid circles mark a family of  $R_k \times 2R_k$  facets at power-of-two multiples of the seed (6.5,2); open circles mark a family of  $R_k \times R_k$  facets. For clarity, the chosen seeds have non-integer coordinates interior to facets. However there exist grid points on the respective facet boundaries that also function as seeds: (7,2) and (3,4).

A family does not necessarily begin with the smallest possible member of its shape class. The largest facet in Figure 2 is a  $5 \times 6$  rectangle of class  $R_{k+1} \times 2R_k$ . the family continues to larger sizes, but begins with the next smaller size, a  $3 \times 4$  ( $R_2 \times 2R_1$ ). This family has

no  $2 \times 2$  ( $R_1 \times 2R_0$ ) member; a  $2 \times 3$  facet sits where that would be expected. The survey revealed no family of this class that does have a  $2 \times 2$  member.

More shape classes might appear beyond the limits of the survey, but that eventuality would surprise me. Every class in (29) is represented in  $G_6$ ; no further classes are represented in  $G_{15}$ .

### 6.1. Family growth

Figure 6 illustrates how magnification and weaving constructs a typical member of a facet family from its predecessor. The lengths of the facet's edges are odd or even according as they take the form  $R_k$  or  $2R_k$  in (29). A coordinate that varies along an odd-length edge has an odd value at one end and even at the other, ordered consistently in successive members. A coordinate that varies along an even-length edge has an odd value at both ends.

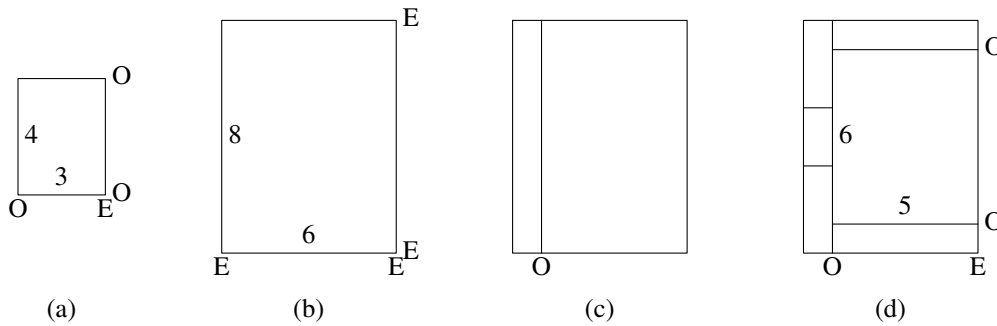


Figure 6. Construction of a facet-family member. (a) Member ( $3 \times 4$ ) of a family of  $R_{k+1} \times 2R_k$  facets. (b) Image of (a) doubled per (1) and (3). (c) Same as (b) with odd verticals drawn. (d) Same as (c) with odd horizontals drawn to make the next facet ( $5 \times 6$ ) in the family. Certain even and odd verticals and horizontals are labeled E and O respectively.

In the magnified image of the predecessor, all edges have even coordinates. Weaving odd verticals slices off one unit along each edge that is an image of an odd vertical. Then weaving odd horizontals slices off one unit along each edge that is an image of an odd horizontal. Other odd horizontals have gaps in the new facet and “ladder rung” bars within each vertical slice.

In every facet family a ladder of as many rungs as will fit flanks at least one vertical side of all but the first member of the family.

### 7. Local symmetry

$G$  exhibits fractal behavior, of which facet families are one manifestation. Another, shown in Figure 7, is *trains* of similar rectangular areas with like local symmetry. Successive elements of a train double in size and location relative to the origin. Symmetries associated with the indicated trains are listed in Table 2.

Trains may overlap. In Figure 7 trains 1 and 2 are nested. Trains 4 and 5 together make a train with symmetry about a horizontal axis.

Train 2 arises from periodicity. Duplicate trains necessarily begin at successive periods, making an infinite spray (in the horticultural sense) of such trains. Periodicity similarly

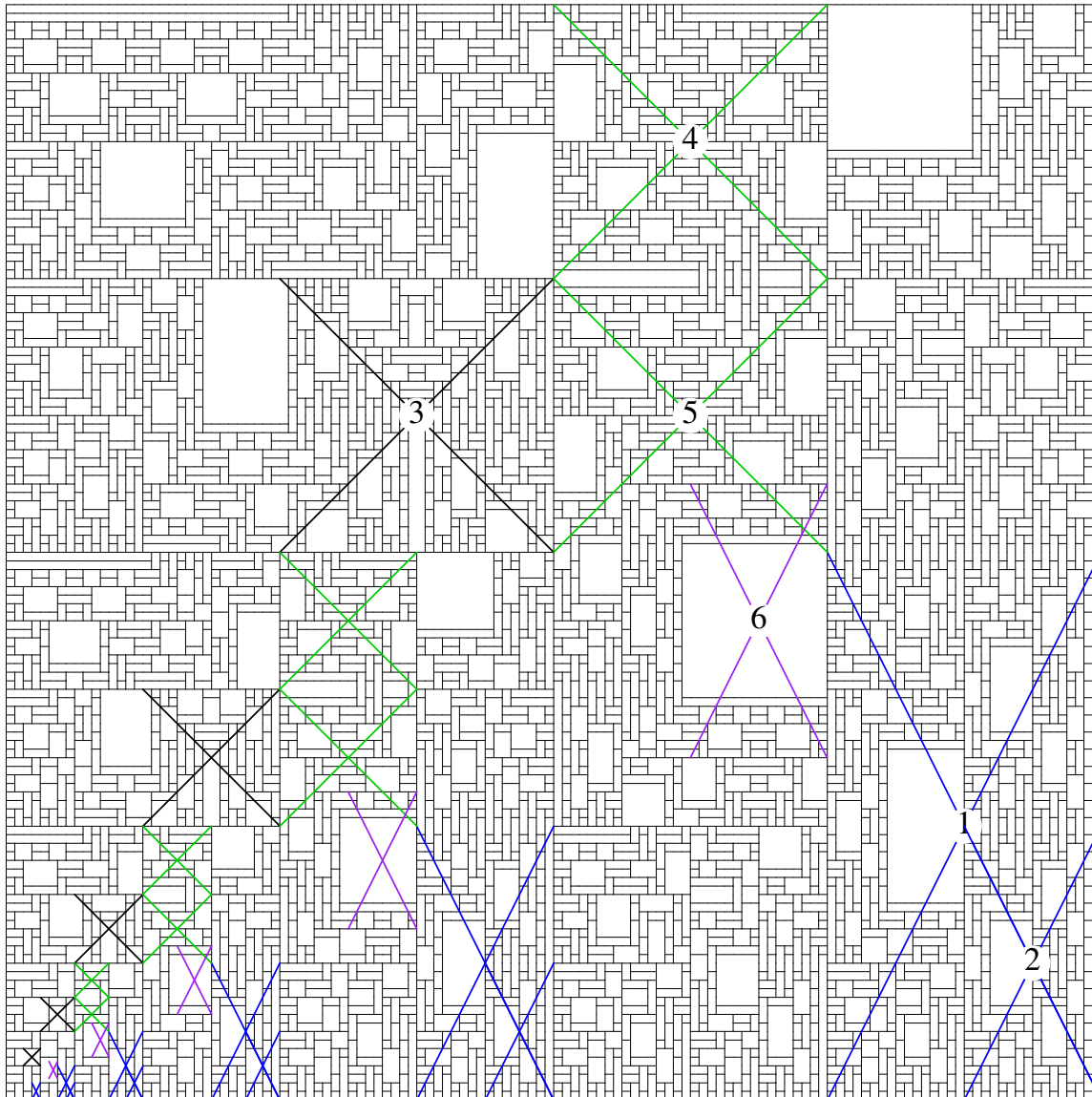


Figure 7. Fractal behavior in  $G_7$ . Rectangle of consistent symmetry type are indicated by trains of rectangles spanned by X's. The train number is shown in the largest member of each train; trains are shown in color where available. Symmetry does not always attain on rectangle boundaries.

produces sprays for all trains, not just train 1.

Rectangles of train 1 have further fractal properties. Two copies of each rectangle make up the right half of its successor. Thus branches of the spray bifurcate at each doubling in size. Another bifurcating sub-pattern, seen to the left of the large central rectangle in both train 1 and train 6, becomes more vivid in further train members. A similar motif appears in other trains, too.

Each member of train 6 can be extended 1/2 its width to the left to make a train with symmetry about a horizontal axis, or 1/4 its height at top and bottom to make a train with symmetry about a vertical axis.

Table 2. Symmetry types of trains marked in Figure 7. Dimensions of a train member are given in terms of the least  $i$  for which  $G_i$  contains the member.

Train	Width	Height	Axis of symmetry		Central Symmetry
			Horizontal	Vertical	
1 (large blue)	$2^{i-2}$	$2^{i-1}$		✓	
2 (small blue)	$2^{i-3}$	$2^{i-2}$		✓	
3 (black)	$2^{i-2}$	$2^{i-2}$	✓		
4 (upper green)	$2^{i-2}$	$2^{i-2}$			✓
5 (lower green)	$2^{i-2}$	$2^{i-2}$			✓
6 (purple)	$2^{i-3}$	$2^{i-2}$	✓	✓	✓

We now examine trains of one symmetry class in more detail. Much of the analysis involves the mid-line of a rectangle. If the mid-line does not lie on a horizontal, doubling places the mid-line of the successor rectangle on a horizontal. If a mid-line lies on an odd horizontal, doubling places the successor mid-line on an even horizontal. All mid-lines thereafter lie on even horizontals. An even-horizontal mid-line can contain no bars, for the switch of parity on an odd vertical that encountered the bar would destroy symmetry.

When constructing the successor of a rectangle in a train symmetrical about a bar-free horizontal, doubling preserves symmetry. Then weaving odd verticals preserves symmetry. To preserve symmetry in the final step of weaving odd horizontals, each pair of horizontals placed symmetrically about the mid-line must “start off on the same foot” within the rectangle. I do not know why this last property holds for most trains in Figure 7. For the blue-marked rectangles, however, the property follows from the fact that every horizontal crosses a ruler tick; see Section 5. This synchronizes the gaps in each symmetric pair of of odd horizontals.

Thus the existence of infinite trains is attested by train 1 and its spray.

### 7.1. Color symmetry

Color symmetries map attribute values—in the present case values of  $v$  and  $h$ —as well as positions. A train with a kind of color symmetry originates on a vertical centerline at  $i = 6$  on the bottom edge of  $G$ . The centerline of the  $m^{\text{th}}$  member of the train, where  $m \geq 0$ , occurs at  $i = 6 \cdot 2^m$ ; its height is  $2^{m+3}$ . Horizontal segments incident on a centerline are centrally symmetric about the point  $(6 \cdot 2^m, 2^{m+2})$ .

$$h(6 \cdot 2^m - 1, j) = h(6 \cdot 2^m, 2^{m+3} - j) \quad (30)$$

Verticals that weave across these segments have central color symmetry; bars map to gaps and vice versa, as illustrated in Figure 8.

$$v(6 \cdot 2^m - 1, j) = v(6 \cdot 2^m + 1, 2^{m+3} - j - 1) + 1 \quad (31)$$

According to (1), magnified images of these verticals occur at  $i = 6 \cdot 2^{m+1} \pm 2$ . They retain central color symmetry. Repeated magnification flanks each centerline with exponentially spaced color-symmetric companions.

$$v(6 \cdot 2^m - 2^k, j) = v(6 \cdot 2^m + 2^k, 2^{m+3} - j - 1) + 1, \quad 0 \leq k \leq m$$

Another color-symmetric train can be obtained by the transpose-and-stretch transformation. Partial trains contained in a particular slab can be transformed by translations appropriate to that slab per the periodicity theorem. Thus the color-symmetric pattern at 6 recurs with period 8, at 14, 22, 30, ...

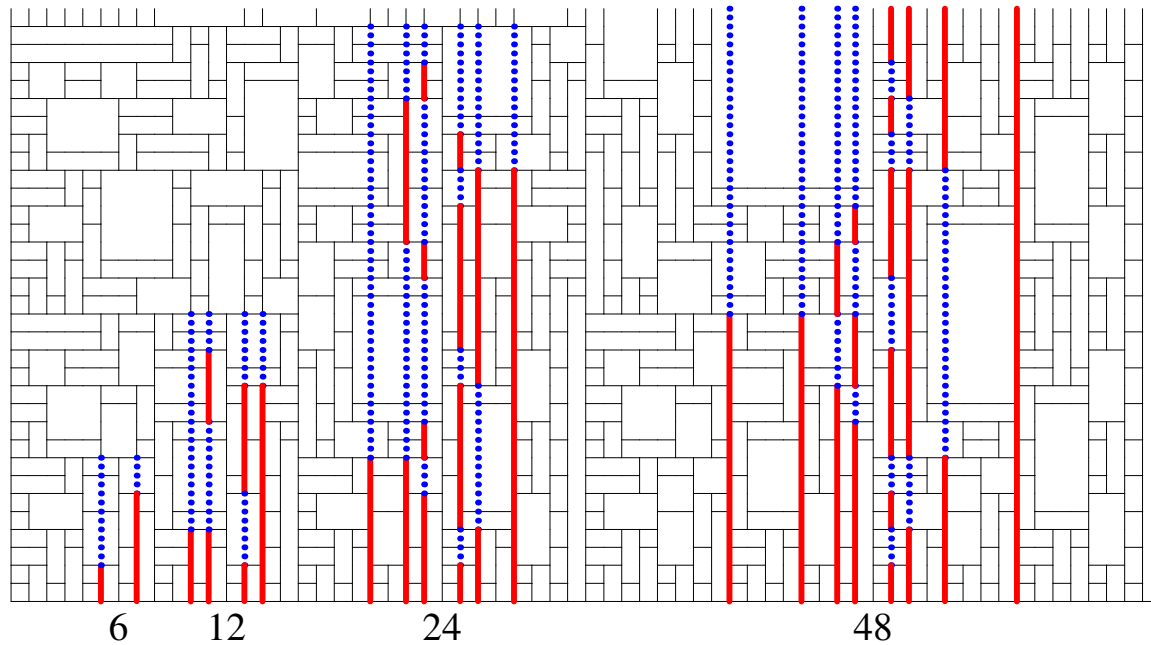


Figure 8. Labeled verticals are midlines of members of a train of groups of color-symmetric vertical segments. Heavy bars (drawn in red if color is available) on one vertical correspond to gaps indicated by heavy dotted lines (blue) on a mated vertical read in the opposite direction. Color-symmetric verticals centered at 48 are truncated at just over half their actual height.

## 8. What next?

The grail of <https://oeis.org/A328080> remains elusive: a formula for the number of facets in  $G_n$ . Another desideratum is formulas for  $v(i, j)$  and  $h(i, j)$ , very likely in terms of the bits of the binary representation of  $i$  and  $j$ . A solution to the latter problem could well serve as a stepping-stone to the former.

One also hopes that less tedious proofs can be found, especially for Section 4. The formulation in Section 3.1 is tantalizing. Can  $H_n$  be shown to be the left half of  $G_n$  more directly, without the algebra of Section 3?

The observations of Sections 6 and 7 suggest further questions. Is the inventory of shape classes complete? Are all facet families infinite? How do rectangular patches of symmetry arise? Why do they form trains? What aspect ratios can they have? Do color-symmetric trains unrelated to those described in Section 7.1 exist?

## 9. Acknowledgements

Neil Sloane introduced me to the Conant gasket and conjectured several of its properties, thus giving me a fascinating puzzle to chew on. Peter McIlroy noticed various parity properties that play important roles in the periodicity proof.

**Bibliography**

- [OEIS] *Online Encyclopedia of Integer Sequences*, <https://oeis.org>  
[C99] *Programming Languages – C*, ISO/IEC 9899 (1999)